Mesons in (2+1)-dimensional light front QCD: Investigation of a Bloch effective Hamiltonian

Dipankar Chakrabarti* and A. Harindranath†
Saha Institute of Nuclear Physics, 1/AF, Bidhan Nagar, Calcutta 700064 India
(Received 4 May 2001; published 28 September 2001)

We study the meson sector of (2+1)-dimensional light front QCD using a Bloch effective Hamiltonian in the first nontrivial order. The resulting two-dimensional integral equation is converted into a matrix equation and solved numerically. We investigate the efficiency of Gaussian quadrature in achieving the cancellation of linear and logarithmic light front infrared divergences. The vanishing energy denominator problem, which leads to severe infrared divergences in 2+1 dimensions, is investigated in detail. Our study indicates that in the context of Fock space based effective Hamiltonian methods to tackle gauge theories in 2+1 dimensions, approaches such as the similarity renormalization method may be mandatory due to uncanceled infrared divergences caused by the vanishing energy denominator problem. We define and numerically study a reduced model which is relativistic, free from infrared divergences, and exhibits logarithmic confinement. The manifestation and violation of rotational symmetry as a function of the coupling are studied quantitatively.

DOI: 10.1103/PhysRevD.64.105002 PACS number(s): 11.10.Ef, 11.10.St, 11.15.Tk, 12.38.Lg

I. INTRODUCTION AND MOTIVATION

There are various well-known motivations [1] to study QCD in the light front Hamiltonian formalism. In fact, there have been many attempts recently to study the relativistic bound state problem in the Hamiltonian formalism in a light front Fock space basis (for a review, see Ref. [2]). It has been realized that a major impediment to a straightforward diagonalization of the Hamiltonian is the rapid growth of the dimension of the Hamiltonian matrix with the particle number. An alternative approach will be to use an *effective* Hamiltonian that operates on a few particle basis. A challenging problem here is that, for a successful description of low energy observables, the effective Hamiltonian must incorporate the main features of strong interaction dynamics.

One of the first attempts invoked the Tamm-Dancoff [3] or Bloch-Horowitz effective Hamiltonian. Though it was successful in tackling (1+1)-dimensional gauge theories, its deficiencies became apparent when attempts were made in 3+1 dimensions. First and foremost of these is the lack of confinement in the case of QCD. Second is the appearance of the bound state eigenvalue in the energy denominators. This has two undesirable consequences. First, a light front singularity of the type $1/k^+$, where k^+ is the light front longitudinal momentum of the exchanged gluon, remains in the bound state equation, which would have been canceled if free energies appeared in the energy denominators. Second, from the fermion self-energy contribution, in addition to the mass divergence another ultraviolet divergence appears (for an example in the context of (3+1)-dimensional Yukawa model see Ref. [4]) which contributes to the renormalization of the coupling. This contribution is also infrared divergent, and can be identified as arising from fermion wave function renormalization. It is the Fock space truncation that has produced this unphysical divergence which would otherwise have been canceled by vertex renormalization in a strict order by order perturbative calculation.

It is well known that various standard formulas for the effective Hamiltonian all have drawbacks. Some of the deficiencies of the Bloch-Horowitz formalism are absent in the Bloch effective Hamiltonian [5], which was reinvented in the context of renormalization group by Wilson [6]. The Bloch Hamiltonian has two desired properties, namely, the effective Hamiltonian is (1) Hermitian and (2) involves only unperturbed energies in the energy denominator. Use of the Bloch effective Hamiltonian eliminates two major problems of the Tamm-Dancoff approach to gauge theories mentioned above. However, the Bloch effective Hamiltonian has an undesirable feature, namely, the vanishing energy denominator. To the best of our knowledge, the Bloch effective Hamiltonian was never assessed in terms of its strengths and weaknesses in the study of bound state problems in field theory.

In the study of bound states, QCD poses challenging problems. To overcome many pitfalls of standard effective Hamiltonians, a similarity renormalization was proposed [7]. This avoids vanishing energy denominators, and thus provides an improvement over the Bloch effective Hamiltonian. Initial attempts in the similarity renormalization approach worked in either the nonrelativistic limit [8] or the heavy quark effective theory context [9]. Only recently has work begun [10] to address many practical problems, especially the numerical ones one faces in this approach.

A major feature of gauge theories on the light front is severe light front infrared divergences of the type $1/(k^+)^2$, where k^+ is the exchanged gluon longitudinal momentum which appears in instantaneous four-fermion, two-fermion two-gluon, and four-gluon interactions. In old-fashioned perturbation theory these divergences are canceled by transverse gluon interactions. In similarity perturbation theory the cancellation is only partial, and singular interactions survive. Before embarking on a detailed study of effective Hamiltonian in the similarity renormalization approach, which is a modification of the Bloch effective Hamiltonian, it is quite instructive to study the Bloch effective Hamiltonian itself. The result of such a study can serve as a benchmark against which one can evaluate the merits of the similarity renormal-

*Email address: dipankar@theory.saha.ernet.in
†Email address: hari@theory.saha.ernet.in

ization scheme. This will also provide us with quantitative measures of the strengths and weaknesses of numerical procedures in handling singular interactions (in the context of light front field theory) on the computer. It is crucial to have such quantitative measures in order to study the effects of similarity cutoff factors on the nature of the spectrum. This is one of the motivations of the present work.

Just as in the Tamm-Dancoff or Bloch-Horowitz formalism, the Bloch effective Hamiltonian of QCD in the first nontrivial order also does not exhibit confinement in $3+1$ dimensions. Since one of our major concerns is the study of spectra for confining interactions, we go to $2+1$ dimensions. In this case, in the limit of heavy fermion mass, a logarithmic confining potential emerges. There are several other reasons to study light front QCD in $2+1$ dimensions. They arise from both theoretical and computational issues which we discuss next.

First of all, issues related to ultraviolet divergence become more complicated in the light front approach, since power counting is different [1] on the light front. We obtain products of ultraviolet and infrared divergent factors which complicate the renormalization problem. Going to two-space, one-time dimensions greatly simplifies this issue due to the absence of ultraviolet divergences except in mass corrections. An extra complication is that Fock space truncation introduces extra ultraviolet divergences which complicate the situation in nonperturbative bound state computations [4]. Such special divergences do not occur in $2+1$ dimensions. A third complication one faces in $3+1$ dimensions is that, on enlarging the Fock space in a bound state calculation, one soon faces the running of the coupling constant. At low energy scales, the effective coupling grows, resulting in a strongly coupled theory [11] making the weak coupling approach with a perturbatively determined Hamiltonian unsuitable or making it mandatory to invent mechanisms such as the nonzero gluon mass to stop the drastic growth [1]. In $(2+1)$-dimensional QCD we do not face this problem, since the coupling constant is dimensionful in this superrenormalizable field theory and does not run due to ultraviolet divergence. We *can keep* the coupling arbitrarily small and study the structure of the bound states in a weakly coupled theory.

Second, in $1+1$ dimensions, in the gauge $A^+=0$, dynamical gluons are absent and their effect is felt only through instantaneous interactions between fermions. Further, recall that in light front theory, vacuum is trivial. As a result, the Fock space structure of the bound states is remarkably simple. For example, the ground state meson is just a $q\bar{q}$ pair at both weak and strong couplings. In contrast, in $2+1$ dimensions, one component of the gauge field remains dynamical and one can systematically study the effects of dynamical gluons. Also note that $2+1$ dimensions are the lowest dimensions where glueball states are possible, and offers one an opportunity to study their structure in the Fock space language without additional complications of $3+1$ dimensions.

A third reason deals with aspects of rotational symmetry. $2+1$ dimensions offer the first opportunity to investigate violations of Lorentz invariance introduced by various cutoffs (momenta and/or particle number) in the context of bound state calculations. This is to be contrasted with $1+1$ dimensions, where the sole Lorentz generator, namely, boost, is kinematical in light front field theory. Since in $2+1$ dimensions we have a superrenormalizable field theory, violations introduced by transverse momentum cutoffs are minimal. Thus, in contrast to $3+1$ dimensions, one can study violations caused by a truncation of the particle number alone and by longitudinal momentum cutoffs. It is also conceivable that one can enlarge the Fock space sector and investigate its effect on restoring Lorentz invariance. It is expected that such investigations are more viable in $2+1$ dimensions compared to $3+1$ dimensions due to less severe demand on computational resources.

A fourth reason concerns the similarity renormalization approach. In $3+1$ dimensions it has been shown that the similarity renormalization group approach [7] to effective Hamiltonian in QCD leads to logarithmic confining interaction [12]. It is of interest to investigate corresponding effective Hamiltonians in $2+1$ dimensions, especially since the canonical Hamiltonian already leads to logarithmic confinement in the nonrelativistic limit in this case. It is also known that in $3+1$ dimensions the confining part of the effective Hamiltonian violates rotational symmetry. Does the violation of rotational symmetry occur also in $2+1$ dimensions? If so, how does it manifest itself?

In this work we initiate a systematic study of light front QCD in $2+1$ dimensions to investigate the various issues discussed above. The plan of the rest of this paper is as follows: In Sec. II we present the canonical Hamiltonian of $(2+1)$-dimensional QCD. The Bloch effective Hamiltonian in the $q\bar{q}$ sector in the lowest nontrivial order is derived in Sec. III, and the bound state equation is derived. The divergence structure is discussed in detail in Sec. IV. In Sec. V we numerically investigate the cancellation of light front linear infrared divergences and the consequences of the vanishing energy denominator problem, which leads to *uncanceled* infrared divergences in the bound state equation. A model which is relativistic, free from infrared divergences, and exhibits logarithmic confinement is presented in Sec. VI. In Sec. VII we present a numerical investigation of this model in the weak coupling limit. In this section, we also discuss the violation of rotational symmetry in this model at strong coupling. Finally Sec. VIII contains a discussion and conclusions. Since the Bloch effective Hamiltonian is unfamiliar to most of the readers, we present a detailed derivation in Appendix A. Details of the numerical procedures used in this work are given in Appendix B.

II. CANONICAL HAMILTONIAN

In this section we present the canonical light front Hamiltonian of $(2+1)$-dimensional QCD. The Lagrangian density is given by

$$\mathcal{L}=[-\tfrac{1}{4}(F_{\lambda\sigma a})^2+\bar{\psi}(\gamma^\lambda iD_\lambda-m)\psi], \tag{2.1}$$

with

$$iD^{\mu}=\frac{1}{2}i\overleftrightarrow{\partial^{\mu}}+gA^{\mu},$$

$$F^{\mu\lambda a}=\partial^{\mu}A^{\lambda a}-\partial^{\lambda}A^{\mu a}+gf^{abc}A^{\mu b}A^{\lambda c}. \tag{2.2}$$

We have the equations of motion,

$$[i\gamma^{\mu}\partial_{\mu}+g\gamma^{\mu}A_{\mu}-m]\psi=0, \tag{2.3}$$

$$\partial_{\mu}F^{\mu\nu a}+gf^{abc}A_{\mu b}F_{c}^{\mu\nu}+g\bar{\psi}\gamma^{\nu}T^{a}\psi=0. \tag{2.4}$$

Because we are in 2+1 dimensions, we immediately face an ambiguity since there are no γ matrices in 2+1 dimensions. In the literature both two component [13] and four component [14] representations have been used. For simplicity, we pick the two component representation. Explicitly,

$$\gamma^{0}=\sigma_{2}=\begin{pmatrix}0 & -i\\ i & 0\end{pmatrix},\quad \gamma^{1}=i\sigma_{3}=\begin{pmatrix}i & 0\\ 0 & -i\end{pmatrix},$$

$$\gamma^{2}=i\sigma_{1}=\begin{pmatrix}0 & i\\ i & 0\end{pmatrix}, \tag{2.5}$$

$$\gamma^{\pm}=\gamma^{0}\pm\gamma^{2},\quad \gamma^{+}=\begin{pmatrix}0 & 0\\ 2i & 0\end{pmatrix},\quad \gamma^{-}=\begin{pmatrix}0 & -2i\\ 0 & 0\end{pmatrix}, \tag{2.6}$$

$$\Lambda^{\pm}=\frac{1}{4}\gamma^{\mp}\gamma^{\pm},\quad \Lambda^{+}=\begin{pmatrix}1 & 0\\ 0 & 0\end{pmatrix},\quad \Lambda^{-}=\begin{pmatrix}0 & 0\\ 0 & 1\end{pmatrix}. \tag{2.7}$$

The fermion field operator $\psi^{\pm}=\Lambda^{\pm}\psi$. We have

$$\psi^{+}=\begin{pmatrix}\xi\\ 0\end{pmatrix},\quad \psi^{-}=\begin{pmatrix}0\\ \eta\end{pmatrix} \tag{2.8}$$

where ξ and η are one component fields. We choose the light front gauge $A^{+a}=0$. From the equation of motion, we obtain the equation of constraint

$$i\partial^{+}\psi^{-}=[\alpha^{1}(i\partial^{1}+gA^{1})+\gamma^{0}m]\psi^{+}. \tag{2.9}$$

Thus the fermion constrained field is

$$\eta=\frac{1}{\partial^{+}}[-(i\partial^{1}+gA^{1})+im]\xi. \tag{2.10}$$

From the equation of motion, in the gauge $A^{+a}=0$, we have the equation of constraint

$$-\frac{1}{2}(\partial^{+})^{2}A^{-a}=-\partial^{1}\partial^{+}A^{1a}-gf^{abc}A^{1b}\partial^{+}A^{1c}-2g\xi^{\dagger}T^{a}\xi. \tag{2.11}$$

Using the equations of constraint, we eliminate ψ^{-} and A^{-} in favor of dynamical fields ψ^{+} and A^{1}, and arrive at the canonical Hamiltonian given by

$$H=H_{0}+H_{int}=\int dx^{-}dx^{1}(\mathcal{H}_{0}+\mathcal{H}_{int}). \tag{2.12}$$

The free Hamiltonian density is given by

$$\mathcal{H}_{0}=\xi^{\dagger}\frac{-(\partial^{1})^{2}+m^{2}}{i\partial^{+}}\xi+\frac{1}{2}\partial^{1}A^{1a}\partial^{1}A^{1a}. \tag{2.13}$$

The interaction Hamiltonian density is given by

$$\mathcal{H}_{int}=\mathcal{H}_{1}+\mathcal{H}_{2}, \tag{2.14}$$

with

$$\begin{aligned}\mathcal{H}_{1}=&g\xi^{\dagger}A^{1}\frac{\partial^{1}}{\partial^{+}}\xi+g\xi^{\dagger}\frac{\partial^{1}}{\partial^{+}}(A^{1}\xi)-gm\xi^{\dagger}A^{1}\frac{1}{\partial^{+}}\xi\\ &+gm\xi^{\dagger}\frac{1}{\partial^{+}}(A^{1}\xi)-2g\frac{1}{\partial^{+}}(\partial^{1}A^{1a})\xi^{\dagger}T^{a}\xi\\ &+gf^{abc}\partial^{1}A^{1a}\frac{1}{\partial^{+}}(A^{1b}\partial^{+}A^{1c})\end{aligned} \tag{2.15}$$

and

$$\begin{aligned}\mathcal{H}_{2}=&-2g^{2}\xi^{\dagger}T^{a}\xi\left(\frac{1}{\partial^{+}}\right)^{2}\xi^{\dagger}T^{a}\xi+g^{2}\xi^{\dagger}A^{1}\frac{1}{\partial^{+}}(A^{1}\xi)\\ &+2g^{2}f^{abc}\frac{1}{\partial^{+}}(\xi^{\dagger}T^{a}\xi)\frac{1}{\partial^{+}}(A^{1b}\partial^{+}A^{1c})\\ &+\frac{1}{2}g^{2}f^{abc}f^{ade}\frac{1}{\partial^{+}}(A^{1b}\partial^{+}A^{1c})\frac{1}{\partial^{+}}(A^{1d}\partial^{+}A^{1e}).\end{aligned} \tag{2.16}$$

The one component fermion field is given by

$$\xi(x^{+}=0,x^{-},x^{1})=\int\frac{dk^{+}dk^{1}}{2(2\pi)^{2}\sqrt{k^{+}}}[b(k)e^{-ik\cdot x}+d^{\dagger}(k)e^{ik\cdot x}]. \tag{2.17}$$

The Fock operators obey the anticommutation relations

$$\begin{aligned}\{b(k),b^{\dagger}(q)\}&=2(2\pi)^{2}k^{+}\delta^{2}(k-q),\\ \{d(k),d^{\dagger}(q)\}&=2(2\pi)^{2}k^{+}\delta^{2}(k-q),\end{aligned} \tag{2.18}$$

other anticommutators being zero. Note that in the two component representation, light front fermions do not carry helicity in 2+1 dimensions.

In free field theory, the equation of motion of the dynamical field A^{1} is the same as that of a free massless scalar field [15], and hence we can write

$$\begin{aligned}&A^{1}(x^{+}=0,x^{-},x^{1})\\ &\quad=\int\frac{dk^{+}dk^{1}}{2(2\pi)^{2}k^{+}}[a(k)e^{-ik\cdot x}+a^{\dagger}(k)e^{ik\cdot x}].\end{aligned} \tag{2.19}$$

The Fock operators obey the commutation relation

$$[a(k),a^{\dagger}(q)]=2(2\pi)^2k^+\delta^2(k-q), \tag{2.20}$$

other commutators being zero.

We substitute the Fock expansions [Eqs. (2.17) and (2.19)] into the Hamiltonian, and treat all terms as normal ordered. Thus we arrive at the canonical Hamiltonian in the Fock basis.

III. BLOCH EFFECTIVE HAMILTONIAN IN THE MESON SECTOR AND THE BOUND STATE EQUATION

In this section we evaluate the Block effective Hamiltonian to the lowest nontrivial order for a meson state, and derive the effective bound state equation. We define the P space to be the $q\overline{q}$ sector of the Fock space, and the Q space to be the rest of the space. In the lowest nontrivial order, the Bloch effective Hamiltonian is given by (see Appendix A for details)

$$\langle i|H_{eff}|j\rangle=\langle i|(H_0+H_{int})|j\rangle+\frac{1}{2}\sum_k\ \langle i|v|k\rangle\langle k|v|j\rangle \times\left[\frac{1}{\epsilon_i-\epsilon_k}+\frac{1}{\epsilon_j-\epsilon_k}\right]. \tag{3.1}$$

States $|i\rangle$ and $|j\rangle$ are, explicitly,

$$|a\rangle=b^{\dagger}(p_1,\alpha)d^{\dagger}(p_2,\alpha)|0\rangle,$$
$$|b\rangle=b^{\dagger}(p_3,\beta)d^{\dagger}(p_4,\beta)|0\rangle, \tag{3.2}$$

where p_1 and p_2 denote momenta and α and β denote colors which are summed over. Explicitly, $p_1=(p_1^+,p_1^1)$ etc., where p_1^+ is the plus component and p_1^1 is the transverse component. For simplicity of notation, we will denote the transverse component of momenta without the superscript 1.

The free part of the Hamiltonian leads to the matrix element

$$\langle a|H|b\rangle=\left[\frac{m^2+p_1^2}{p_1^+}+\frac{m^2+p_2^2}{p_2^+}\right]2(2\pi)^2p_1^+\delta^2(p_1-p_3) \times2(2\pi)^2p_2^+\delta^2(p_2-p_4)\delta_{\alpha\beta}. \tag{3.3}$$

From the four fermion interaction, we obtain the contribution

$$-4g^2(T^aT^a)_{\alpha\alpha}\frac{1}{(p_1^+-p_3^+)^2}2(2\pi)^2\sqrt{p_1^+p_2^+p_3^+p_4^+}\,\delta^2 \times(p_1+p_2-p_3-p_4)\delta_{\alpha\beta}. \tag{3.4}$$

Next we evaluate the contribution from the second order term. The intermediate state $|k\rangle$ is a quark, antiquark, gluon state. This intermediate state gives rise to both self-energy and gluon exchange contributions. The self-energy contributions are

$$g^2C_f\delta_{\alpha\beta}p_1^+2(2\pi)^2\delta^2(p_1-p_3)p_2^+2(2\pi)^2\delta^2(p_2-p_4)\int\frac{dk_1^+dk_1}{2(2\pi)^2(p_1^+-k_1^+)}\left\{-2\frac{(p_1-k_1)}{(p_1^+-k_1^+)}+\frac{k_1}{k_1^+}+\frac{p_1}{p_1^+}-i\frac{m}{k_1^+}+i\frac{m}{p_1^+}\right\}$$
$$\times\frac{1}{ED_1}\left\{-2\frac{(p_1-k_1)}{(p_1^+-k_1^+)}+\frac{k_1}{k_1^+}+\frac{p_1}{p_1^+}+i\frac{m}{k_1^+}-i\frac{m}{p_1^+}\right\}+g^2C_f\delta_{\alpha\beta}p_1^+2(2\pi)^2\delta^2(p_1-p_3)p_2^+2(2\pi)^2\delta^2(p_2-p_4)$$
$$\times\int\frac{dk_2^+dk_2}{2(2\pi)^2(p_2^+-k_2^+)}\left\{-2\frac{(p_2-k_2)}{(p_2^+-k_2^+)}+\frac{k_2}{k_2^+}+\frac{p_2}{p_2^+}-i\frac{m}{k_2^+}+i\frac{m}{p_2^+}\right\}\frac{1}{ED_2}\left\{-2\frac{(p_2-k_2)}{(p_2^+-k_2^+)}+\frac{k_2}{k_2^+}+\frac{p_2}{p_2^+}+i\frac{m}{k_2^+}-i\frac{m}{p_2^+}\right\}, \tag{3.5}$$

with

$$ED_1=\frac{p_1^2+m^2}{p_1^+}-\frac{m^2+k_1^2}{k_1^+}-\frac{(p_1-k_1)^2}{(p_1^+-k_1^+)}\quad,\quad ED_2=\frac{p_2^2+m^2}{p_2^+}-\frac{m^2+k_2^2}{k_2^+}-\frac{(p_2-k_2)^2}{(p_2^+-k_2^+)}\quad. \tag{3.6}$$

The gluon exchange contributions are

$$-g^2(T^aT^a)_{\alpha\alpha}2(2\pi)^2\delta^2(p_1+p_2-p_3-p_4)\sqrt{p_1^+p_2^+p_3^+p_4^+}\left\{-2\frac{(p_1-p_3)}{(p_1^+-p_3^+)}+\frac{p_3}{p_3^+}+\frac{p_1}{p_1^+}-i\frac{m}{p_3^+}+i\frac{m}{p_1^+}\right\}$$
$$\times\left\{-2\frac{(p_1-p_3)}{(p_1^+-p_3^+)}+\frac{p_2}{p_2^+}+\frac{p_4}{p_4^+}+i\frac{m}{p_2^+}-i\frac{m}{p_4^+}\right\}\frac{1}{2}\frac{\theta(p_1^+-p_3^+)}{(p_1^+-p_3^+)}\left\{\frac{1}{\frac{m^2+p_4^2}{p_4^+}-\frac{(p_1-p_3)^2}{(p_1^+-p_3^+)}-\frac{m^2+p_2^2}{p_2^+}}\right.$$
$$\left.+\frac{1}{\frac{m^2+p_1^2}{p_1^+}-\frac{(p_1-p_3)^2}{(p_1^+-p_3^+)}-\frac{m^2+p_3^2}{p_3^+}}\right\}-g^2(T^aT^a)_{\alpha\alpha}2(2\pi)^2\delta^2(p_1+p_2-p_3-p_4)\sqrt{p_1^+p_2^+p_3^+p_4^+}$$

$$\times\left\{-2\frac{(p_3-p_1)}{(p_3^+-p_1^+)}+\frac{p_3}{p_3^+}+\frac{p_1}{p_1^+}-i\frac{m}{p_3^+}+i\frac{m}{p_1^+}\right\}\left\{-2\frac{(p_3-p_1)}{(p_3^+-p_1^+)}+\frac{p_2}{p_2^+}+\frac{p_4}{p_4^+}+i\frac{m}{p_2^+}-i\frac{m}{p_4^+}\right\}\frac{1}{2}\frac{\theta(p_3^+-p_1^+)}{(p_3^+-p_1^+)}$$

$$\times\left\{\frac{1}{\frac{m^2+p_2^2}{p_2^+}-\frac{(p_3-p_1)^2}{(p_3^+-p_1^+)}-\frac{m^2+p_4^2}{p_4^+}}+\frac{1}{\frac{m^2+p_3^2}{p_3^+}-\frac{(p_3-p_1)^2}{(p_3^+-p_1^+)}-\frac{m^2+p_1^2}{p_1^+}}\right\}. \tag{3.7}$$

After the construction of H_{eff} in the two particle space, we proceed as follows. Consider the bound state equation

$$H_{eff}|\Psi\rangle=\frac{M^2+P^2}{P^+}|\Psi\rangle, \tag{3.8}$$

where P^+, P, and M are the longitudinal momentum, the transverse momentum, and the invariant mass of the state, respectively. The state $|\Psi\rangle$ is given by

$$|\Psi\rangle=\sum_\beta\int\frac{dp_3^+dp_3}{\sqrt{2(2\pi)^2p_3^+}}\int\frac{dp_4^+dp_4}{\sqrt{2(2\pi)^2p_4^+}}\phi_2(P;p_3,p_4)$$
$$\times b^\dagger(p_3,\beta)d^\dagger(p_4,\beta)|0\rangle\sqrt{2(2\pi)^2P^+}\,\delta^2(P-p_3-p_4), \tag{3.9}$$

which we represent symbolically as

$$|\Psi\rangle=\sum_j\phi_{2j}|j\rangle. \tag{3.10}$$

Taking projection with the state $\langle i|=\langle 0|d(p_2,\alpha)b(p_1,\alpha)$, we obtain the effective bound state equation

$$\frac{M^2+P^2}{P^+}\phi_{2i}=H_{0i}\phi_{2i}+\sum_j\langle i|H_{Ieff}|j\rangle\phi_{2j}. \tag{3.11}$$

We introduce the internal momentum variables (x,k) and (y,q) via $p_1^+=xP^+$, $p_1=xP+k$, $p_2^+=(1-x)P^+$, $p_2=(1-x)P-k$, $p_3^+=yP^+$, $p_3=yP+q$, $p_4^+=(1-y)P^+$, $p_4=(1-y)P-q$ and the amplitude $\phi_2(P;p_1,p_2)=(1/\sqrt{P^+})\psi_2(x,k)$.

The fermion momentum fractions x and y range from 0 to 1. To handle end point singularities, we introduce the cutoff $\eta\leqslant x,y\leqslant 1-\eta$. This does not prevent the gluon longitudinal momentum fraction $x-y$ from becoming zero, and we introduce the regulator δ such that $|x-y|\geqslant\delta$. To regulate ultraviolet divergences, we introduce the cutoff Λ on the relative transverse momenta k and q. We remind the reader that in the superrenormalizable field theory under study, only ultraviolet divergence is in the fermion self-energy contribution, which we remove by a counterterm before discretization.

The bound state equation is

$$\left[M^2-\frac{m^2+k^2}{x(1-x)}\right]\psi_2(x,k)$$
$$=\mathcal{S}\psi_2(x,k)-4\frac{g^2}{2(2\pi)^2}C_f\int dydq\,\psi_2(y,q)\frac{1}{(x-y)^2}$$
$$-\frac{g^2}{2(2\pi)^2}C_f\int dydq\,\psi_2(y,q)\frac{1}{2}\frac{V}{ED}. \tag{3.12}$$

The self-energy contribution is

$$\mathcal{S}=-\frac{g^2}{2(2\pi)^2}C_f\int_0^x dy\int dqxy$$
$$\times\frac{\left[\left(\frac{q}{y}+\frac{k}{x}-\frac{2(k-q)}{(x-y)}\right)^2+\frac{m^2(x-y)^2}{x^2y^2}\right]}{(ky-qx)^2+m^2(x-y)^2}$$
$$-\frac{g^2}{2(2\pi)^2}C_f\int_x^1 dy\int dq(1-x)(1-y)$$
$$\times\frac{\left[\left(\frac{q}{1-y}+\frac{k}{1-x}+\frac{2(q-k)}{(y-x)}\right)^2+\frac{m^2(y-x)^2}{(1-x)^2(1-y)^2}\right]}{[k(1-y)-q(1-x)]^2+m^2(x-y)^2}. \tag{3.13}$$

The boson exchange contribution is

$$\frac{V}{ED}=\frac{\theta(x-y)}{(x-y)}\left[\frac{1}{\frac{m^2+q^2}{y}+\frac{(k-q)^2}{(x-y)}-\frac{m^2+k^2}{x}}\right.$$
$$\left.+\frac{1}{\frac{m^2+k^2}{1-x}+\frac{(k-q)^2}{x-y}-\frac{m^2+q^2}{1-y}}\right][K(k,x,q,y)+iV_I]$$
$$+\frac{\theta(y-x)}{(y-x)}\left[\frac{1}{\frac{m^2+k^2}{x}+\frac{(q-k)^2}{(y-x)}-\frac{q^2+m^2}{y}}\right.$$
$$\left.+\frac{1}{\frac{m^2+q^2}{1-y}+\frac{(q-k)^2}{y-x}-\frac{m^2+k^2}{1-x}}\right][K(q,y,k,x)+iV_I], \tag{3.14}$$

where

$$K(k,x,q,y)=\left(\frac{q}{y}+\frac{k}{x}-2\frac{(k-q)}{(x-y)}\right)\left(\frac{q}{1-y}+\frac{k}{1-x}+\frac{2(k-q)}{(x-y)}\right)-\frac{m^2(x-y)^2}{xy(1-x)(1-y)}, \tag{3.15}$$

$$V_I=-\frac{m}{xy(1-x)(1-y)}[q(2-y-3x)+k(3y+x-2)]. \tag{3.16}$$

IV. DIVERGENCE STRUCTURE

In this subsection we carry out a detailed analysis of the divergence structure of the effective bound state equation. We encounter both infrared and ultraviolet divergences.

A. Ultraviolet divergences

First we consider ultraviolet divergences. In the super-renormalizable field theory under consideration, with terms appearing in the canonical Hamiltonian as normal ordered, ultraviolet divergence is encountered only in the self-energy contributions. To isolate the ultraviolet divergence, we re-write the self-energy integrals as

$$\mathcal{S}=-\frac{g^2}{2(2\pi)^2}C_f\int_0^x dy\int_{-\Lambda}^{+\Lambda}dq\left[\frac{(x+y)^2}{xy(x-y)^2}-\frac{4m^2}{(ky-qx)^2+m^2(x-y)^2}\right]-\frac{g^2}{2(2\pi)^2}C_f\int_x^1 dy\times\int_{-\Lambda}^{+\Lambda}dq\left[\frac{(2-x-y)^2}{(y-x)^2(1-x)(1-y)}-\frac{4m^2}{[k(1-y)-q(1-x)]^2+m^2(x-y)^2}\right]. \tag{4.1}$$

The first term inside the square brackets in the above equation is ultraviolet divergent, which we cancel by adding an ultraviolet counterterm given by

$$\mathcal{C}=+\frac{g^2}{2(2\pi)^2}C_f\int_{-\Lambda}^{+\Lambda}dq\left[\int_0^x dy\frac{(x+y)^2}{xy(x-y)^2}+\int_x^1 dy\frac{(2-x-y)^2}{(y-x)^2(1-x)(1-y)}\right]. \tag{4.2}$$

After the addition of this counterterm, the bound state equation is ultraviolet finite.

B. Infrared divergences

The infrared divergences that appear in the bound state equation are of two types: (1) light front infrared divergences that arise from the gluon longitudinal momentum fraction $x_g=0$, and (2) true infrared divergences that arise from gluon transverse momentum $k_g=0$ and gluon longitudinal momentum fraction $x_g=0$.

1. Cancellation of light front infrared divergences in the effective bound state equation

First consider light front infrared divergences. The effective bound state equation [Eq. (3.12)] explicitly has a linear light front infrared divergent term $1/(x-y)^2$ coming from the instantaneous gluon exchange. The most divergent part of the numerator of the transverse gluon exchange term in this equation is $-4[(k-q)^2/(x-y)^2]$. After combining the terms, the linear infrared divergent term is completely canceled and the resultant effective bound state equation takes the form

$$\left[M^2-\frac{m^2+k^2}{x(1-x)}\right]\psi_2(x,k)=\mathcal{S}1\,\psi_2(x,k)-\frac{g^2}{2(2\pi)^2}C_f\int dy\,dq\,\psi_2(y,q)\times\frac{1}{2}\left[\frac{\tilde{V}_1}{E_1}+\frac{\tilde{V}_2}{E_2}+iV_I\left(\frac{1}{E_1}+\frac{1}{E_2}\right)\right]. \tag{4.3}$$

The self-energy contribution, made ultraviolet finite by the addition of the counterterm is

$$\mathcal{S}1=+\frac{g^2}{2(2\pi)^2}C_f\int_0^x dy\int_{-\Lambda}^{+\Lambda}dq\frac{4m^2}{(ky-qx)^2+m^2(x-y)^2}+\frac{g^2}{2(2\pi)^2}C_f\int_x^1 dy\int_{-\Lambda}^{+\Lambda}dq\times\frac{4m^2}{[k(1-y)-q(1-x)]^2+m^2(x-y)^2}. \tag{4.4}$$

The energy denominator factors are

$$\frac{1}{E_1}=\frac{xy}{[ky-qx]^2+m^2(x-y)^2},$$

$$\frac{1}{E_2}=\frac{(1-x)(1-y)}{[k(1-y)-q(1-x)]^2+m^2(x-y)^2}. \tag{4.5}$$

The vertex terms are

$$\tilde{V}_1=\theta(x-y)\tilde{U}(k,x,q,y)+\theta(y-x)\tilde{U}(q,y,k,x), \tag{4.6}$$

$$\tilde{V}_2=\theta(x-y)\tilde{U}(k,1-x,q,1-y)+\theta(y-x)\times\tilde{U}(q,1-y,k,1-x), \tag{4.7}$$

with

$$\tilde{U}(k,x,q,y)=4\frac{m^2}{xy}-\frac{m^2(x-y)^2}{xy(1-x)(1-y)}+\frac{q^2}{y(1-y)}+\frac{k^2}{x(1-x)}$$
$$-2\frac{k^2}{(x-y)}\frac{1}{x(1-x)}+2\frac{q^2}{(x-y)}\frac{1}{y(1-y)}$$
$$+\frac{kq}{x(1-y)}+\frac{kq}{y(1-x)}$$
$$+2\frac{kq}{(x-y)}\left[\frac{1-2y}{y(1-y)}-\frac{1-2x}{x(1-x)}\right]. \tag{4.8}$$

In addition to the $1/x_g^2$ singularity, which is canceled, transverse gluon exchange contributions also contain a $1/x_g$ singularity which is removed by the principal value prescription. The cancellation of this singularity is an appealing feature of the Bloch effective Hamiltonian, in contrast to the Tamm-Dancoff effective Hamiltonian where the singularity cancellation does not occur because of the presence of invariant mass in the energy denominator [16].

2. "True" infrared divergences

Next we consider true infrared divergences. Consider the self-energy integrals. The energy denominators in these expressions vanish when $k=q$ and $x=y$, which correspond to vanishing gluon momentum. By carrying out the integrals explicitly, in the limit $\Lambda\to\infty$ we obtain,

$$\mathcal{S}1=\frac{mg^2}{2\pi}C_f\left[\frac{1}{x}\ln\frac{x}{\delta}+\frac{1}{1-x}\ln\frac{1-x}{\delta}\right]. \tag{4.9}$$

Thus the singular part of the self-energy is

$$\mathcal{S}1_{singular}=-\frac{mg^2}{2\pi}C_f\frac{1}{x(1-x)}\ln\delta. \tag{4.10}$$

The infrared divergent contribution from the self-energy gives a positive contribution to the fermion mass. It is important to note that the vanishing of the energy denominator is also possible in 3+1 dimensions, but in this case we do not encounter any divergence. It is the peculiarity of 2+1 dimensions that the vanishing energy denominators cause a severe infrared divergence problem.

The same vanishing energy denominators also occur in the one gluon exchange contributions. Let us now consider various terms in the numerator separately. The terms proportional to $4m^2$ arose from the denominator of the transverse gluon exchange. A straightforward calculation shows that this term leads to both finite and infrared divergent contributions. The infrared divergent contribution is given by

$$\frac{mg^2}{2\pi}C_f\frac{1}{x(1-x)}\ln\delta, \tag{4.11}$$

which exactly cancels the infrared divergent contribution from the self-energy. The finite part, in the nonrelativistic limit, can be shown to give rise to a logarithmically confining potential. Next we have to consider the remaining terms in the numerator. The rest of the terms proportional to m^2 are multiplied by $(x-y)^2$, so that they do not lead to an infrared divergence problem. The numerator of the imaginary part vanishes at $k=q$ and $x=y$, and hence is also infrared finite. It is easy to verify that the rest of the (transverse momentum dependent) terms in the numerator do not vanish when the denominator vanishes; hence the resulting bound state equation is inflicted with infrared divergences arising from the vanishing energy denominator. This problem was first noted in the context of QED in 2+1 dimensions by Tam, Hamer, and Yung [17], but was not investigated by these authors. We remind the reader that this is a peculiarity of 2+1 dimensions, which provides us with a unique opportunity to explore the consequences of the vanishing energy denominator problem.

V. NUMERICAL STUDY OF THE BOUND STATE EQUATION

We convert the integral equation into a matrix equation with the use of Gaussian quadrature. (For details of the numerical procedure, see Appendix B.) C_f is set to 1 for all numerical calculations presented. As mentioned above, an important feature of gauge theories on the light front is the presence of linear infrared divergences. They appear in the canonical Hamiltonian in the instantaneous four fermion interaction term. When the qqg states are integrated out *completely* in perturbation theory, they also appear in the effective four fermion interaction and cancel each other out. Noncancellation of this divergence is a major feature of similarity renormalization approach. We first address the issue of how linear divergences manifest themselves in the nonuniform grid of the Gaussian quadrature, and how well they can handle linear light front infrared divergence. We have studied numerically discretized versions of Eq. (3.12) where the divergences are present separately in the discretized version together with the counterterm given in Eq. (4.2). For $g=0.2$, we have calculated eigenvalues with and without the instantaneous interaction. The results, presented in Fig. 1(a) for the lowest eigenvalue shows, that the Gaussian quadrature can handle the cancellation very efficiently.

After the cancellation of the linear light front infrared divergence, a logarithmic infrared divergence which arises from the vanishing energy denominator survives in the bound state equation. Here we have to distinguish two types of terms. In the first type, the coefficient of the logarithmic infrared divergence is independent of the fermion transverse momentum; in the second type, the coefficient is dependent on the momentum. Self-energy and Coulomb interactions are of the first type. In the weak coupling limit, since the wave function is dominated by a very low transverse momentum, we anticipate that contributions of the second type will be dynamically suppressed even though both are multiplied by the same coupling constant. This is especially true of any discrete grid, which automatically imposes a lower limit on the smallest longitudinal momentum fraction allowed. Thus, at weak coupling, even if there are uncanceled infrared divergences (divergences of the second type), they may not be numerically significant, whereas divergences of the second type are significant. By switching the self-energy contribu-

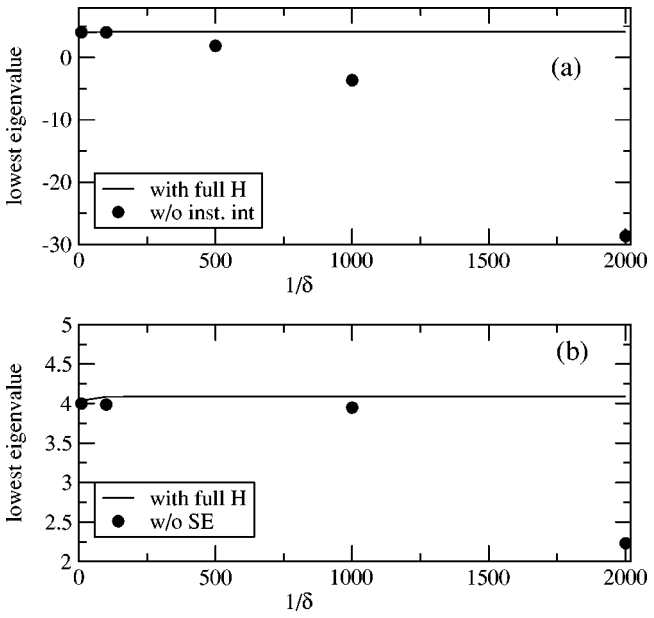

FIG. 1. Cancellation of the linear infrared divergence. The full line denotes the full Hamiltonian. (a) shows the cancellation of the light front infrared divergence by switching the instantaneous interaction on and off. Filled circles indicate there is no instantaneous interaction. (b) shows the cancellation of logarithmic infrared divergence by switching on and off the self energy term. Filled circles indicate there is no self energy. The parameters are $g=0.2$, $\eta=0.00001$, $m=1$, $\kappa=20$, $n_1=40$, and $n_2=50$.

tion off and on, we have studied this interplay. The lowest eigenvalue with and without self-energy contribution is plotted in Fig. 1(b). This shows the cancellation of the dominant logarithmic infrared divergence. Since there are still uncanceled infrared divergences in the bound state equation (with coefficients proportional to the fermion transverse momenta) this figure further illustrates the fact that such divergences are not numerically significant at weak coupling.

As the strength of the interaction grows, the wave function develops medium to large transverse momentum components, and the infrared catastrophe triggered by the vanishing energy denominator becomes manifest numerically. This is illustrated in Table I, where we present the variation with δ of the first five eigenvalues for two different choices of the coupling g. The table clearly shows that on a discrete grid, the uncanceled infrared divergences due to the vanishing energy denominator problem are not numerically significant at weak coupling; however, their effect is readily felt at a stronger coupling.

VI. REDUCED MODEL

In this section we consider a model Hamiltonian free from infrared divergences, constructed by dropping the transverse momentum dependent terms from the numerator of the effective Hamiltonian. For convenience, we further drop the terms proportional to $(x-y)^2$ and the imaginary part. This defines our reduced model, which is also ultraviolet finite. The equation governing the model is given by

$$\left[M^2-\frac{m^2+k^2}{x(1-x)}\right]\psi_2(x,k)=\mathcal{S}1\,\psi_2(x,k)+\mathcal{B}. \tag{6.1}$$

The self-energy contribution $\mathcal{S}1$ is the same as given in Eq. (4.4). The boson exchange contribution $\mathcal{B}$ is given by

$$\mathcal{B}=-\frac{1}{2}\frac{g^2}{2(2\pi)^2}C_f\int_0^1 dy\int_{-\Lambda}^{+\Lambda}dq\frac{4m^2}{(ky-qx)^2+m^2(x-y)^2}\times\psi_2(y,q)-\frac{1}{2}\frac{g^2}{2(2\pi)^2}C_f\int_0^1 dy\int_{-\Lambda}^{+\Lambda}dq\times\frac{4m^2}{[k(1-y)-q(1-x)]^2+m^2(x-y)^2}\psi_2(y,q). \tag{6.2}$$

Again we discretize Eq. (6.1) by the Gaussian quadrature. The convergence of the eigenvalues as a function of the number of grid points is presented in Table II. In this table we also present the (in)dependence of eigenvalues on the momentum cutoff.

$2+1$ dimensions provide an opportunity to study the manifestation and violation of rotational symmetry in light front field theory in a simpler setting compared to $3+1$ dimensions. The absence of spin further facilitates this study. Rotational symmetry in this case simply implies degeneracy with respect to the sign of the azimuthal quantum number l. Thus we expect all $l\neq 0$ states to be twofold degenerate. By a suitable change of variables, one can easily show that our

TABLE I. Variation with δ of the full Hamiltonian. The parameters are $n1=40$, $n2=50$, $\eta=0.00001$, and $\kappa=20.0$ in $k=(1/\kappa)\tan(u\pi/2)$.

g	δ	Eigenvalues (M^2)				
	0.00001	4.0913	4.1113	4.1122	4.1181	4.1209
	0.0001	4.0913	4.1113	4.1122	4.1181	4.1209
0.2	0.001	4.0913	4.1113	4.1122	4.1181	4.1209
	0.005	4.0901	4.1066	4.1099	4.1100	4.1112
	0.01	4.0870	4.0972	4.0972	4.0973	4.0973
	0.0001	−187230.4	−187225.4	−186664.9	−186664.8	−31506.9
0.6	0.001	−187230.4	−187225.4	−186664.9	−186664.8	−31506.9
	0.005	1.9094	1.9415	3.1393	3.1399	4.5697
	0.01	4.5735	4.7337	4.7667	4.7832	4.8277

TABLE II. Convergence of eigenvalues with $n1$ and $n2$ (reduced model). The parameters are $m=1.0$, $g=0.2$, and $\eta=0.00001$.

$n1$	$n2$	Eigenvalues (lowest five) ($\kappa=10.0$)				
20	20	4.08926	4.10605	4.10768	4.11061	4.11085
30	30	4.09045	4.10909	4.11038	4.11516	4.11699
40	30	4.09045	4.10913	4.11035	4.11524	4.11697
40	40	4.09102	4.11052	4.11154	4.11711	4.11951
40	50	4.09136	4.11133	4.11222	4.11811	4.12096
50	50	4.09136	4.11135	4.11219	4.11816	4.12095
50	60	4.09158	4.11188	4.11263	4.12189	4.12290
46	60	4.09158	4.11187	4.11264	4.11877	4.12189
46	66	4.09168	4.11212	4.11284	4.11905	4.12231
46	74	4.09179	4.11237	4.11305	4.11934	4.12276
$n1$	$n2$	Eigenvalues (lowest five) ($\kappa=20.0$)				
46	74	4.09179	4.11240	4.11301	4.11940	4.12273

reduced model in the nonrelativistic limit reduces to Schrödinger equation in two space dimensions with a logarithmic confining potential. In the weak coupling limit, since C_f is set to 1, we can compare our results of the reduced model (where we do not make any nonrelativistic approximation) with the spectra obtained in nonrelativistic $(2+1)$-dimensional QED (QED_{2+1}). Tam *et al.* [17] solved the radial Schrödinger equation in momentum space for $l=0$ states, and Koures [18] solved the coordinate space radial Schrödinger equation for general l. Since we are solving the light front bound state equation, rotational symmetry is not at all manifest. However, at weak coupling we expect that the spectra exhibit rotational symmetry to a very good approximation. Our numerical results are compared with those of Koures in Table III for two values of the coupling. At $g=0.2$ we find reasonable agreement with the degeneracy in the spectrum. Even at $g=0.6$ the violation of the rotational symmetry is very small. The splittings of levels which are supposed to be degenerate become more visible at very strong coupling, as can be seen from Table IV for $g=5$.

Along with the eigenvalues, the diagonalization process also yields wave functions. We have plotted wave-functions corresponding to the first four eigenvalues in Fig. 2 as a function of x and k. All wave functions are normalized to $\int_0^1 dx \int dk \psi^2(x,k)=1$. The lowest state is nodeless and corresponds to $l=0$. The next two states correspond to $l=1$ and have one node. It is interesting to note how the node appears in wave functions which correspond to degenerate levels. Since the rotational symmetry cannot be manifest in the variables x and k, how can the wave functions still indicate this? From Fig. 2, it is clear that the way this problem is resolved is by one wave function having a node in k and the other wave function having a node in x. Thus, even if we did not know about the underlying symmetry from other means, the light front wave functions have a subtle way of indicating the symmetry.

VII. SUMMARY, DISCUSSION, AND CONCLUSIONS

In light front Hamiltonian approach to the bound state problem in gauge theories, the Bloch effective Hamiltonian has certain advantages compared to the Tamm-Dancoff or Bloch-Horowitz formalisms. Furthermore, the recently proposed similarity renormalization approach is a modification of the Bloch approach. In order to estimate the impact of similarity form factors in the similarity renormalization approach quantitatively, it is extremely useful to have a quantitative study of the bound state problem in Bloch formalism. As far as we know, the Bloch effective Hamiltonian has never been investigated in the context of the bound state problem in light front field theory.

To avoid complexities due to ultraviolet divergences we turn to $2+1$ dimensions. This allows us to investigate light front infrared divergences in the bound state problem in the presence of transverse dynamics without the additional complication arising from the mixing of ultraviolet and light front infrared divergences. Further, $2+1$ dimensions allow us to study quantitatively the manifestation and possible violation of rotational symmetry in light front theory in a simpler setting. The emergence of a logarithmic confining interaction in the limit of heavy fermion masses is an added impetus to study gauge theories in $2+1$ dimensions.

Only very recently has a study begun of the various issues that arise in numerical computations in the similarity approach. Since the similarity renormalization approach is a modification of the Bloch effective Hamiltonian approach, a detailed numerical study of the latter can serve as a benchmark against which one can evaluate the merits of the similarity approach. It is also important to evaluate the strengths and weaknesses of numerical procedures quantitatively in

TABLE III. Reduced model. The parameters are $n1=46$, $n2=74$, $\eta=0.00001$, $m=1.0$. $k=\tan(q\pi/2)/\kappa$, and $\kappa=20.0$. Eigenvalues within parentheses are $\pm l$ degenerate (broken) states.

g		Eigenvalues		
	This	4.0918	(4.1124, 4.1130)	4.1194
0.2	work	(4.1227, 4.1235)	(4.1268, 4.1273)	(4.1298, 4.1303)
	Koures	4.0925 ($l=0$)	4.1144 ($l=1$)	4.1214 ($l=0$)
	(Ref. [18])	4.1260 ($l=2$)	4.1303 ($l=1$)	4.1340 ($l=3$)
	This	4.5856	(4.7741, 4.7821)	4.8390
0.6	work	(4.8767, 4.8816)	(4.9094, 4.9184)	(4.9458, 4.9481)
	Koures	4.5806 ($l=0$)	4.7777 ($l=1$)	4.8409 ($l=0$)
	(Ref. [18])	4.8827 ($l=2$)	4.9205 ($l=1$)	4.9545 ($l=3$)

TABLE IV. The first few eigenvalues in the reduced model. The parameters are $g=5.0$, $m=1.0$, and $\eta=0.00001$. (I) Parametrization $k=u\Lambda m/[(1-u^2)\Lambda+m]$, $\Lambda=40.0$. (II) Parametrization $k=\tan(u\pi/2)/\kappa$, $\kappa=10.0$. Eigenvalues within parentheses are $\pm l$ degenerate (broken) states.

	$n1$	$n2$	Eigenvalues					
I	40	50	18.217	(30.702, 33.499)	35.206	(39.955, 41.159)	(41.332, 43.271)	(44.134, 45.272)
	46	70	18.276	(30.774, 33.616)	35.318	(40.106, 41.331)	(41.483, 43.477)	(44.375, 45.503)
II	40	50	18.980	(31.507, 34.219)	35.826	(40.406, 41.888)	(41.921, 43.788)	(44.345, 45.163)
	46	70	19.008	(31.542, 34.319)	35.935	(40.626, 42.031)	(42.088, 44.010)	(44.647, 45.780)

handling singular interactions in the context of light front dynamics on the computer.

In this work we have focused on the Gaussian quadrature (GQ), which is one straightforward procedure to solve the integral equation by converting it into a matrix equation. We have demonstrated the efficiency of the GQ method in handling linear and logarithmic light front infrared divergences.

A major advantage of the similarity approach is that it avoids the vanishing energy denominator problem that is present in the Bloch formalism. In $2+1$ dimensions the vanishing energy denominator leads to severe *infrared divergences*, and hence we are presented with a unique opportunity to study its consequences. We encounter two types of infrared divergences: (1) one with a coefficient proportional to fermion mass, and (2) another with a coefficient proportional to fermion transverse momentum. The former type is canceled in the bound state equation between fermion dressing by gluons and gluon exchange between fermions. The latter type is uncanceled, but can be dynamically suppressed at very weak coupling on a *finite* grid. We have demonstrated that, on a discrete grid provided by the GQ, the uncanceled divergences are numerically insignificant at weak coupling, whereas the catastrophe due to their presence is readily felt at stronger coupling.

We proceed to study a reduced model that is free from infrared divergences and which reduces to the Schrödinger equation with a logarithmic potential in the nonrelativistic limit. This model provides us with an opportunity to study the simplest manifestation and possible violation of rotational symmetry, in the context of light front field theory. Even though the Hamiltonian does not exhibit rotational symmetry we have shown that at weak coupling spectra exhibit rotational symmetry to a very good approximation. We have also shown that even though the rotational symmetry is not manifest in the variables x and k, light front wave functions have a subtler way of indicating the underlying symmetry.

Our study indicates that in the context of Fock space based effective Hamiltonian methods to tackle gauge theories in $2+1$ dimensions, approaches such as the similarity renormalization method are mandatory due to uncanceled infrared divergences caused by the vanishing energy denominator problem. It is important to recall that a Bloch effective Hamiltonian is generated by completely integrating out the intermediate gluons irrespective of whether they are low or high energy. Is this justified in a confining theory?

Now that we have obtained quantitative measures of the vanishing energy denominator problem and the nature of the spectra at weak coupling of the Bloch effective Hamiltonian, the next step is to study QCD_{2+1} in similarity renormalization approach which avoids the vanishing energy denominator problem. An important issue here is the nature of new effective interactions generated by the similarity approach. It has been shown that in $3+1$ dimensions, similarity approach generates logarithmic confining interactions, which, however, breaks rotational symmetry. It is interesting to investigate the corresponding situation in $2+1$ dimensions.

APPENDIX A: BLOCH PERTURBATION THEORY FOR THE EFFECTIVE HAMILTONIAN

The Bloch perturbation theory was introduced in Ref. [5]. Here we follow the treatment in Ref. [19], where the reader can find many examples of perturbative calculations.

Consider a Hamiltonian H defined at a cutoff Λ. Let us try to lower the cutoff to λ. In general, the cutoff could be in energy and/or particle number. Let us denote by Q an opera-

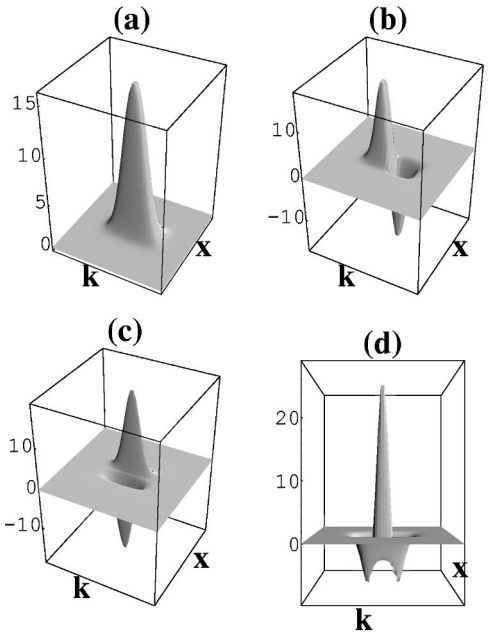

FIG. 2. The wave functions corresponding to the lowest four eigenvalues of the reduced model as functions of x and k. The parameters are $g=0.2$, $\eta=0.00001$, $m=1$, $\kappa=10$, $n_1=46$, and $n_2=74$. (a) Lowest state. (b) First excited state. (c) Second excited state. (d) Third excited state. The first and second excited states should be degenerate in the absence of a violation of rotational symmetry.

tor that projects onto all of the states removed when the cutoff is lowered. Let $P=I-Q$. We have

$$Q^2=Q, \quad P^2=P, \quad PQ=QP=0. \tag{A1}$$

Our purpose is to find an effective Hamiltonian H_{eff} that produces the same eigenvalues in the subspace P as the original Hamiltonian H.

We introduce an operator R that satisfies

$$Q|\psi\rangle=RP|\psi\rangle \tag{A2}$$

for all eigenstates of the Hamiltonian that have support in the subspace P. R gives the part of $|\psi\rangle$ outside the space projected by P in terms of the part of $|\psi\rangle$ inside the space. We require that R does not act on states outside the subspace. This means that $R=RP$, $R=QR$, and $R^2=0$. From $R=QR$, we have $PR=0$. Also note that $R^\dagger \neq R$.

We start from the set of equations

$$PHP|\psi\rangle+PHQ|\psi\rangle=EP|\psi\rangle, \tag{A3}$$

$$QHP|\psi\rangle+QHQ|\psi\rangle=EQ|\psi\rangle. \tag{A4}$$

From Eq. (A3),

$$RPHP|\psi\rangle+RPHQRP|\psi\rangle=ERP|\psi\rangle. \tag{A5}$$

From Eq. (A4),

$$QHP|\psi\rangle+QHQRP|\psi\rangle=ERP|\psi\rangle. \tag{A6}$$

Subtracting,

$$RH_{PP}-H_{QQ}R+RH_{PQ}R-H_{QP}=0. \tag{A7}$$

We have introduced the notations $PHP=H_{PP}$, and so on. We put $H=h+v$ with $[h,Q]=0$. Then

$$Rh_{PP}-h_{QQ}R-v_{QP}+Rv_{PP}-v_{QQ}R+Rv_{PQ}R=0, \tag{A8}$$

which shows that R starts first order in v.

We start from the eigenvalue equation

$$H(P+Q)|\psi\rangle=E(P+Q)|\psi\rangle. \tag{A9}$$

i.e.,

$$H(P+R)P|\psi\rangle=E(P+R)P|\psi\rangle. \tag{A10}$$

Multiplying from the left by $(P+R^\dagger)$, we have

$$(P+R^\dagger)H(P+R)P|\psi\rangle=E(P+R^\dagger)(P+R)P|\psi\rangle. \tag{A11}$$

Using $PR=0$, $R^\dagger P=0$, $(P+R^\dagger)(P+R)=P+R^\dagger R$. Thus we can rewrite the eigenvalue equation as

$$\left[\frac{1}{1+R^\dagger R}\right]^{1/2}(P+R^\dagger)H(P+R)\left[\frac{1}{1+R^\dagger R}\right]^{1/2} \times[1+R^\dagger R]^{1/2}P|\psi\rangle=E[1+R^\dagger R]^{1/2}P|\psi\rangle, \tag{A12}$$

i.e.,

$$H_{eff}|\phi\rangle=E|\phi\rangle, \tag{A13}$$

where

$$|\phi\rangle=[1+R^\dagger R]^{1/2}P|\psi\rangle \tag{A14}$$

and

$$H_{eff}=\left[\frac{1}{1+R^\dagger R}\right]^{1/2}(P+R^\dagger)H(P+R)\left[\frac{1}{1+R^\dagger R}\right]^{1/2}. \tag{A15}$$

Our next task is to generate a perturbative expansion. We denote free eigenstates in P by $|a\rangle$, $|b\rangle$, etc. We denote free eigenstates in Q by $|i\rangle$, $|j\rangle$, etc. Then

$$h_{PP}|a\rangle=\epsilon_a|a\rangle,$$

$$h_{QQ}|i\rangle=\epsilon_i|i\rangle. \tag{A16}$$

Let us compute R to lowest orders in the perturbation theory. Let us write $R=R_1+R_2+\cdots$, where the subscript denotes orders in v. A straightforward calculation leads to

$$\langle i|R_1|a\rangle=\frac{\langle i|v_{QP}|a\rangle}{\epsilon_a-\epsilon_i}, \tag{A17}$$

$$\langle i|R_2|a\rangle=-\sum_b \frac{\langle b|v|a\rangle\langle i|v|b\rangle}{(\epsilon_a-\epsilon_i)(\epsilon_b-\epsilon_i)}+\sum_j \frac{\langle i|v|j\rangle\langle j|v|a\rangle}{(\epsilon_a-\epsilon_i)(\epsilon_a-\epsilon_j)}. \tag{A18}$$

Our next task is to develop a perturbation theory expansion for the effective Hamiltonian to a given order.

We start from the expression for the effective Hamiltonian. Remember that $R_1\sim O(v)$ and $R_2\sim O(v^2)$.

To order v, $H_{eff}=PHP$, and hence

$$\langle a|H_{eff}|b\rangle=\langle a|(h+v)|b\rangle. \tag{A19}$$

To second order in v, we have

$$H_{eff}=[1-\tfrac{1}{2}R^\dagger R][PHP+PHR+R^\dagger HP+R^\dagger HR] \times[1-\tfrac{1}{2}R^\dagger R]. \tag{A20}$$

From $R^\dagger HR$ we obtain,

$$\langle a|R^\dagger HR|b\rangle=\sum_i \epsilon_i\frac{\langle a|v|i\rangle\langle i|v|b\rangle}{(\epsilon_a-\epsilon_i)(\epsilon_b-\epsilon_i)}. \tag{A21}$$

From PHR and $R^\dagger HP$ terms we obtain

$$\sum_i \langle a|H|i\rangle\langle i|R_1|b\rangle + \sum_i \langle a|R_1^\dagger|i\rangle\langle i|H|b\rangle \quad \text{(A22)}$$

$$= \sum_i \left[\frac{\langle a|v|i\rangle\langle i|v|b\rangle}{\epsilon_a - \epsilon_i} + \frac{\langle a|v|i\rangle\langle i|v|b\rangle}{\epsilon_b - \epsilon_i} \right]. \quad \text{(A23)}$$

From the *normalization factors* we obtain

$$-\frac{1}{2}R^\dagger RPHP - \frac{1}{2}PHPR^\dagger R = -\frac{1}{2}(\epsilon_a + \epsilon_b)\sum_i \frac{\langle a|v|i\rangle\langle i|v|b\rangle}{(\epsilon_a - \epsilon_i)(\epsilon_b - \epsilon_i)}. \quad \text{(A24)}$$

Adding everything, to second order, we have

$$\langle a|H_{eff}|b\rangle = \frac{1}{2}\sum_i \langle a|v|i\rangle\langle i|v|b\rangle \left[\frac{1}{\epsilon_a - \epsilon_i} + \frac{1}{\epsilon_b - \epsilon_i} \right]. \quad \text{(A25)}$$

If $a = b$, this expression reduces to the familiar second order energy shift.

Why is the Bloch formalism preferred over the Bloch-Horowitz formalism? In the former, eigenstates of the effective Hamiltonian are orthonormalized projections of the original eigenstates. In the latter, they are not.

We consider two orthonormalized eigenstates of the original Hamiltonians $|\psi_1\rangle$ and $|\psi_2\rangle$ with $\langle\psi_1|\psi_2\rangle = 0$. However, $P|\psi_1\rangle$ and $P|\psi_2\rangle$ need not be orthogonal, i.e., $\langle\psi_1|PP|\psi_2\rangle = \langle\psi_1|P|\psi_2\rangle \neq 0$. We consider

$$\langle\psi_1|\psi_2\rangle = \langle\psi_1|P|\psi_2\rangle + \langle\psi_1|Q^2|\psi_2\rangle = \langle\psi_1|P|\psi_2\rangle + \langle\psi_1|P^\dagger R^\dagger RP|\psi_1\rangle. \quad \text{(A26)}$$

We construct $|\tilde{\psi}_1\rangle = [1 + R^\dagger R]^{1/2}P|\psi_1\rangle$ and $|\tilde{\psi}_2\rangle = [1 + R^\dagger R]^{1/2}P|\psi_2\rangle$. Then

$$\langle\tilde{\psi}_1|\tilde{\psi}_2\rangle = \langle\psi_1|P|\psi_2\rangle + \langle\psi_1|PR^\dagger RP|\psi_2\rangle = \langle\psi_1|\psi_2\rangle. \quad \text{(A27)}$$

APPENDIX B: DETAILS OF THE NUMERICAL PROCEDURE

Parametrization: The light front variables are parametrized in the following ways in our numerical calculations. The full k interval is divided into $n1$ quadrature points. k is defined by two different ways. One definition is

$$k = \frac{u\Lambda m}{(1-u^2)\Lambda + m}, \quad \text{(B1)}$$

where Λ is the ultraviolet cutoff and the u's are quadrature points lying between -1 and $+1$, so that k goes from $-\Lambda$ to $+\Lambda$. The other definition is

$$k = \frac{1}{\kappa}\tan\left(\frac{u\pi}{2}\right); \quad \text{(B2)}$$

here κ is a parameter that can be tuned to adjust the ultraviolet cutoff. The second definition [Eq. (B2)] of k is very suitable for weak coupling calculations, where we require that maximum points be concentrated near $k = 0$, and obtain better convergence than the first definition (B1).

The longitudinal momentum fraction x ranges from 0 to 1. We divide all x integrations in our calculations into two parts, x ranging from 0 to 0.5 and x ranging from 0.5 to 1, and discretize each x interval into $n2$ quadrature points with the parametrizations

$$x = \frac{1 + v + 2\eta(1-v)}{4}, \quad \eta \leqslant x \leqslant 0.5, \quad \text{(B3)}$$

$$x = \frac{3 + v - 2\eta(1+v)}{4}, \quad 0.5 \leqslant x \leqslant 1 - \eta, \quad \text{(B4)}$$

where v's are the Gauss quadrature points lying between -1 and $+1$, and $\eta(\to 0)$ is introduced to handle end-point singularities in x as mentioned before.

To handle the infrared diverging terms we put the cutoff $|x-y| \geqslant \delta$, and at the end we take the limit $\delta \to 0$. Numerically, this means that the result should converge as one decreases δ if there is no net infrared divergence in the theory.

Diagonalization: After discretization, solving the integral equation becomes a matrix diagonalization problem. The diagonalization has been performed by using the packed storage *LAPACK* [20] routines *DSPEVX* for the reduced model (real symmetric matrix) and *ZHPEVX* for the full Hamiltonian (Hermitian matrix).

[1] K. G. Wilson, T. S. Walhout, A. Harindranath, W. Zhang, R. J. Perry, and S. D. Głazek, Phys. Rev. D **49**, 6720 (1994).

[2] S. J. Brodsky, H. Pauli, and S. S. Pinsky, Phys. Rep. **301**, 299 (1998). For most recent work on discrete light cone quantization see J. Hiller, "Application of Discrete Light Cone Quantization to Yukawa Theory in Four Dimensions," hep-ph/0010061, and references therein.

[3] R. J. Perry, A. Harindranath, and K. G. Wilson, Phys. Rev. Lett. **65**, 2959 (1990).

[4] S. Głazek, A. Harindranath, S. Pinsky, J. Shigemitsu, and K. Wilson, Phys. Rev. D **47**, 1599 (1993).

[5] C. Bloch, Nucl. Phys. **6**, 329 (1958).

[6] K. G. Wilson, Phys. Rev. D **2**, 1438 (1970).

[7] S. D. Głazek and K. G. Wilson, Phys. Rev. D **48**, 5863 (1993); **49**, 4214 (1994); similar flow equations were proposed by F. Wegner, Ann. Phys. (Leipzig) **3**, 77 (1994).

[8] M. Brisudova and R. Perry, Phys. Rev. D **54**, 1831 (1996); M. Brisudova, R. J. Perry, and K. G. Wilson, Phys. Rev. Lett. **78**, 1227 (1997).

[9] W.-M. Zhang, Phys. Rev. D **56**, 1528 (1997).

[10] B. H. Allen and R. J. Perry, Phys. Rev. D **62**, 025005 (2000); R. D. Kylin, Ph.D. thesis, Ohio State University, 2001, hep-ph/0103129.
[11] S. D. Głazek and K. G. Wilson, Phys. Rev. D **57**, 3558 (1998).
[12] R. J. Perry, in *Hadron Physics '94: Topics on the Structure and Interaction of Hadron Systems*, Proceedings, Gramado, Brazil, edited by V. Hercovitz *et al.* (World Scientific, Singapore, 1995).
[13] K. M. Bitar, Phys. Rev. D **7**, 1184 (1973).
[14] M. Burkardt and A. Langnau, Phys. Rev. D **44**, 1187 (1991).
[15] B. Binegar, J. Math. Phys. **23**, 1511 (1982).
[16] M. Krautgartner, H. C. Pauli, and F. Wolz, Phys. Rev. D **45**, 3755 (1992).
[17] A. Tam, C. J. Hamer, and C. M. Yung, J. Phys. G **21**, 1463 (1995).
[18] V. G. Koures, J. Comput. Phys. **128**, 1 (1996).
[19] R. J. Perry, Ann. Phys. (N.Y.) **232**, 116 (1994); B. D. Jones and R. J. Perry, Phys. Rev. D **55**, 7715 (1997).
[20] E. Anderson *et al.*, *LAPACK Users' Guide*, 3rd ed. (Society for Industrial and Applied Mathematics, Philadelphia, 1999). Available on the internet at the URL: http://www.netlib.org/lapack/lug/index.html.